Title:

Effect of active aluminum on soil phosphorus forms in a forested watershed in Akita, Japan

Authors:

Nanae Hosokawa[12a*], Yuka Ozawa[1], Atsushi Hayakawa[1b], Yuichi Ishikawa[1c], Tadashi Takahashi[1]

1: Department of Biological Environment, Akita Prefectural University, Akita, Japan

2: Present affiliation: Institute for Agro-Environmental Sciences, NARO, 3-1-3 Kannondai, Tsukuba, Ibaraki 305-8604, Japan

a ORCID 0000-0003-2336-0570

b ORCID 0000-0002-5359-3896

c ORCID 0000-0001-7926-5869

***: Corresponding author: hosokawan759@affrc.go.jp, nhosokawa18@gmail.com**

Abstract

Volcanic ash has fallen in a broad area in Japan and contributed to the formation of soil physical and chemical properties as a result of abundant supply of active aluminum (Al). However, the effect of two types of active Al, specifically Al-humus complexes and amorphous minerals, on soil phosphorous (P) forms remains unclear. We investigated soil P fractions in forest soil influenced by volcanic materials. Samples from the top 0–10 and 10–20 cm of the soil at the foot of a slope were collected from Japanese cedar forests in a watershed in Japan. Soil samples were sequentially extracted to obtain operationally defined P fraction: calcium (Ca)-P, Al-P and iron (Fe)-P. The soil samples were extracted to obtain oxalate extractable silicon (Si_o) and Al (Al_o) , and pyrophosphate extractable Al (Al_p) and Fe (Fe_p). Regardless of the sampling location, the dominant soil P form was Fe-P, followed by Al-P and Ca-P. Al-P significantly positively correlated with Si_o while Al-P significantly negatively correlated with Al_p. Si_o and Al_p represent amorphous minerals and Al-humus complexes, respectively. Thus, these results suggested that amorphous minerals increased Al-associated P, while Al-humus complexes decreased Al-associated P. In contrast, the correlation between the concentration of Fe-P and Al_p or Fe_p was significantly positive. Since Al_p and Fe_p represent humus, these results suggested that Al-humus complexes increased humus related P. The different effects of the two active forms of Al may result in distinctive P dynamics in forest ecosystems.

Key words: sequential P extraction, active Al, Al-humus complexes, topography, cedar forest soil

1. Introduction

Phosphorus (P) is an important nutrient that can limit net primary production in terrestrial ecosystems (Vitousek et al., 2010; Elser et al., 2007). Most P in soil exists in forms that are absorbed/adsorbed to oxides, clay and humus, and P availability in soil strongly influences vegetation and soil nutrient status (Crews et al., 1995; Porder et al., 2005). Soil P availability can be estimated by determining the binding strength of the various P compounds, and various sequential P extraction methods have been developed (e.g., Chang and Jackson 1957; Hedley 1982; Kuo 1996). Generally, the phosphate-fixing ability increases in the order of carbonate crystals, crystallized aluminum (Al), iron (Fe) oxides, amorphous Al, and Fe oxides (Brady and Weil 2003). Nevertheless, the chemical fraction method has been criticized as does not separate and detect the specific P form (Barrow et al., 2021) and other approaches such as NMR spectrometry and X-ray absorption spectroscopy have been developed (Kruse et al., 2015), chemical fraction still provides useful information.

Volcanic materials play a significant role in soil P dynamics through the production of active Al by its weathering. The produced minerals exist as amorphous minerals (e.g., allophane and imogolite), and as Al-humus complexes under acidic and organic carbon rich conditions (Shoji, 1993; Takahashi and Dahlgren, 2016). Active Al is operationally determined as follows: Al extracted by acid oxalate (Al_o) represents whole active Al; silicon (Si) extracted by acid oxalate (Si_o) is an indicator of allophane and imogolite; and Al extracted by pyrophosphate (Al_p) represents Al-humus complexes. The composition of active Al results in different chemical features, and Andosols are separated into “non-allophanic Andosols” when dominated by Al-humus complexes and “allophanic Andosols” when dominated by amorphous minerals. For example, the P sorption ability in non-allophanic Andosols are stronger than that in allophanic Andosols (Matsuyama et al., 1999; Saigusa et al., 1991). Volcanic materials also influence the

63 chemical features of a non-volcanic soil like Cambisols, and the soils are provided qualifier “andic”
64 (Obara et al., 2011; WRB, 2014). Such andic forest soils are common in Japan (Imaya et al.,
65 2010a, b) since volcanic ash has fallen in the wide areas (Torii, 1990). The soil carbon (C)
66 concentration was significantly positively correlated with the concentration of active Al in central
67 and western Japan (Imaya et al., 2010b), and the variation of active Al would depend on degree
68 of mixing of soil and volcanic ash (Imaya et al., 2010a). Erosion, movement, and redeposition of
69 soil may change the concentration of the volcanic glasses involved in the intensity of the chemical
70 feature of Andosols (e.g., allophane test and phosphate retention) (Arai et al., 1984).
71 Many previous studies reported that the amount of Fe and Al associated P (i.e., extracted
72 by NaOH) is larger than labile P (i.e., extracted by $NaHCO_3$ or resin) in volcanic soils (Borie &
73 Rubio, 2003, Mukai et al., 2016; Redel et al., 2008, 2016; Satti et l., 2007; Schlesinger et al.,
74 1998). However, the relationship between amorphous minerals and the fractionated P is varied
75 among studies. For example, there were significant positive relationships between Al_o and labile
76 organic P or Fe and Al associated organic P in Chile (Redel et al., 2016) and there was a significant
77 negative relationship between Al_o and labile inorganic P in California, USA (Gu et al., 2020), but
78 there was no significant relationship in Argentina (Satti et al., 2007). In addition, there were
79 significant negative relationships between Al_p and labile or Fe and Al associated P in inorganic
80 and organic forms (Redel et al., 2016) but there was a significant positive relationship between
81 Al_p and labile organic P in Argentina (Satti et al., 2007). A potential explanation for these
82 differences is the Hedley method (Hedley, 1982), which most studies applied to, determines Fe-P
83 and Al-P in one fraction. The origins of Fe or Al associated P in volcanic soil is not the same, so
84 different methods were proposed (e.g., Chang and Jackson 1957; Kuo, 1996; Sekiya, 1970). Here,
85 we used the Sekiya method (Sekiya, 1970) since it has been adapted to Japanese soil that is
86 influenced by volcanic materials. In the Sekiya method, Ca-P is considered as readily soluble P

87 that correlates with Truog-P, Al-P is considered as P related with active Al, especially as clay
88 mineral (Sekiya, 1970), and Fe-P is considered as P related with Fe oxide (Chang and Jackson,
89 1957). The Sekiya method has been widely applied to cropland and grassland in Japan (e.g.,
90 Nakamura et al., 2019; Otani and Ae, 1997; Tani et al., 2010), and studies have shown that
91 allophanic and non-allophanic Andosols have a larger amount of Al-P than Fe-P as a result of the
92 abundant active Al.

93 We conducted the study on a watershed that is expected to show a variation of active Al
94 contents in the soil. However, variation of geology and topography within the watershed can also
95 influence the amount and fraction of soil P. Many previous studies found that significant
96 differences of composition and amount of soil P or soil P dynamics by lithologies (Dieter et al.,
97 2010; Gu et al., 2020; Stahr et al., 2018). Catchment-related hydrologic indices and elevation are
98 significant factor determining distribution of soil TP in a mountainous region (Li et al., 2017;
99 Yuan et al. 2019). Soil movement from upper to lower position in a slope is a factor for P
100 accumulation in agriculture fields (Ni and Zhang 2007). Although some studies reported that
101 effect of lithology on soil properties were larger than topography (e.g., K and Mg: Barthold et al.,
102 2008; P: Mage and Porder, 2013), degree of soil movement and deposition is varied by slope
103 angle and vegetation cover (Wakiyama et al. 2010). This suggest that the degree of the effect of
104 lithology and topography on composition and amount of soil P, consequently soil P dynamics can
105 be different by sites.

106 In this study, we investigated the effects of active Al on the soil P fraction in forest soil
107 influenced by volcanic ash, while considering the influence of geology and topography. We
108 investigated soil P in a watershed consisting of two lithologies (igneous and sedimentary rocks)
109 across an altitude of 80–451 m above sea level. We expected that (1) total P and soil P fraction
110 will be significantly different among the lithologies and topography (i.e., slope angle and

111 elevation) (2) even when considering the geological and topographic factors, Al associated P will
112 significantly increase with an increase in the concentration of active Al and (3) effect of two types
113 of active Al (Al_o and Al_p) on fractionated P will be different.
114
115 **2. Material and Methods**
116 **2.1. Soil sampling**
117 Soil samples were collected from 29 locations in Japanese cedar (*Cryptomeria japonica*) forests
118 covering 894 km^2 of the lake Hachiro watershed (Fig. 1). The watershed consists of two
119 lithological areas (igneous and sedimentary rock) according to Chishitsuzu Navi
120 (https://gbank.gsj.jp/geonavi/geonavi.php#11,40.01246,140.23067), and three soil types (non-
121 allophanic Andosols, NAA; allophanic Andosols, AA; and Brown forest soils, BFS) (Table 1)
122 according to the Japanese soil map (https://soil-inventory.dc.affrc.go.jp/index.html). The soil was
123 classified using the Japanese soil classification system (Obara et al., 2011) and AA, NAA, BFS
124 correspond to silandic Andosols, aluandic Andosols, and Cambisols defined in the World
125 Reference Base for Soil Resources (WRB, 2014), respectively. We determined the soil sampling
126 points using the soil map as a rough indicator for soil type, and selected sites to cover all soil
127 areas: nine points from the NAA area, 12 points from the AA area, and eight points from the BFS
128 area, across the two lithological areas (Table 1). The soils were collected from the foot of the
129 slope to investigate the deposition from the upper slope as well as from the individual headwater
130 catchment to ensure independent sampling. We obtained the elevation, area, and slope angle of
131 the headwater catchment of the sampling points using the GIS software TNTmips (TNTmips
132 2015; Micro Images Inc., Raymond New Hampshire, USA). Further detail of the topography of
133 the study site is described in Hayakawa et al. (2020).
134 The soil was collected using a soil auger (diameter 50 mm; Liner sampler DIK-110C,

Daiki Rika Kogyo Co., Ltd., Saitama, Japan). We collected three cores from each sampling point, and cut each core into two sections: 0–10 and 10–20 cm. The three cores from each depth at each sampling point were mixed and air-dried to constant weight. The soils were then sieved through 2 mm mesh to remove coarse roots and gravel. Air-dry possibly leads to a decrease in amorphous minerals and degradation of microbial P (e.g., Achat et al., 2012; Comfort et al., 1991) and thus our estimates may include the uncertainly.

2.2. Sequential P extraction by the Sekiya method (1970)

Sequential P extraction was conducted by the Sekiya method (Sekiya, 1970). Air-dried soil (0.4 g) was added to 40 mL of 2.5% acetic acid and shaken for 2 h. The solution was filtered into a flask through a paper filter (No.6; Advantec Toyo Kaisha, Ltd, Tokyo, Japan). The residue was washed twice with 20 mL 1 M ammonium chloride and the extracts were added into the flask. P in the extract was determined as available P for plants and referred as to Ca-P according to Sekiya (1970). The residual soil was mixed with 40 mL 1 M ammonium fluoride (NH_4F; pH 7) and shaken for 1 h. The extracted solution was passed through a paper filter and the P in the extract was considered as Al associated P (Al-P). The residual soil was mixed with 20 mL saturated salt solution, and the solution was discarded. We replicated this procedure twice. Finally, the soil residue was mixed with 40 mL 0.1 M sodium hydroxide (NaOH) and shaken for 17 h. The extracted solution was passed through a paper filter, and the P in this extract was considered as Fe related P (Fe-P). We measured inorganic P (Ca-IP, Al-IP, and Fe-IP) and total P (Ca-P, Al-P, and Fe-P) in each extraction, and determined organic P (OP) as the difference between the total P and IP in each extraction (Ca-OP, Al-OP, and Fe-OP). We determined Sekiya total P (Sekiya TP) as the sum of Ca-P, Al-P, and Fe-P. We determined total inorganic phosphorus (TIP) as the sum of Ca-IP, Al-IP, and Fe-IP, and total organic phosphorus (TOP) as the sum of Ca-OP, Al-OP, and

159 Fe-OP.

160 Inorganic and total P in each extraction were determined with the Murphy and Riley
161 method (Murphy and Riley, 1962) using continuous flow colorimetry (QuAAtro 2HR; BLTEC
162 Co Ltd., Osaka, Japan), and the analysis for total P was conducted after persulfate digestion. In
163 the determination of Fe-IP, the extraction was acidified to pH 1.5−2.0 with 1 M H_2SO_4 (extract :
164 H_2SO_4 = 10 : 1 [v / v]) to precipitate humic acid (Sekiya, 1970). We then collected the supernatant
165 and neutralized it with 4 M NaOH and 0.25 M H_2SO_4, using *p*-nitrophenol as a pH indicator. For
166 the measurement of Al-P, we diluted the samples by 30% (v / v) with 0.8 M boric acid to avoid
167 color dulling.

168

169 **2.3. Selective Al, Si and Fe extraction**

170 A 0.4 g of air-dried soil was mixed with 40 mL 0.2 M acid ammonium oxalate (pH 3.0) and shaken
171 for 4 h in the dark. The solution was then passed through a paper filter (No.2, Advantec Toyo
172 Kaisha, Ltd, Tokyo, Japan) and Al, Si, and Fe were measured. We refer to these elements in the
173 extracts as Al_o, Si_o, and Fe_o. A 0.4 g of air-dried soil was mixed with 40 mL 0.1 M pyrophosphate
174 (pH 10.0) and shaken for 16 h. The solution was passed through a paper filter (No.2, Advantec
175 Toyo Kaisha, Ltd, Tokyo, Japan) and Al and Fe were measured. We refer to the Al in this extract
176 as Al_p. We quantified Al, Si, and Fe in the oxalate or pyrophosphate extractions using an atomic
177 emission spectrometer using MP-AES (4210; Agilent Technologies Japan, Ltd., Tokyo, Japan).
178 Al_o represents allophane and imogolite, and Al-humus complexes. Si_o represents allophane and
179 imogolite. Fe_o represents amorphous Fe such as ferrihydrite. Al_p represents Al-humus complexes
180 (Dahlgren and Ugolini, 1991; Parfitt and Kimble., 1989). We calculated Al_o + 1 / 2 Fe_o, and when
181 the value was above 2.0%, the soil agreed to one of the requirements for Andosols (Obara et al.,
182 2011; WRB, 2014). In addition, the mol ratio of Al and Si was calculated as (Al_o − Al_p) / Si_o to

assess the chemical composition of amorphous minerals (Parfitt and Kimble., 1989).

2.4. Other soil chemical properties

Soil pH (H_2O) was measured (dry soil : water = 1 : 2.5) in air-dried soil with a pH meter (HM-25R; HORIBA, Ltd., Kyoto, Japan). We digested soil with nitric and perchloric acids to analyze total P (soil TP) and Ca, Mg, K, and Na contents in the soil cores from 0−10 cm and 10−20 cm depths. Soil TP was determined with the vanadomolybdate acid method (Kuo, 1996) using a spectrophotometer (U-1800, HITACHI, Tokyo, Japan). We calculated the soil TP contents over the whole 0−20 cm core by summing the soil TP concentration in the 0−10 and 10−20 cm cores. We measured Ca, Mg, K, and Na with atomic emission spectrometry using MP-AES. We calculated sum of Ca, Mg, K, and Na content in the whole 0–20 cm soil core by summing the concentrations in the 0–10 and 10 − 20 cm depths. Total C and nitrogen (TC and TN) concentrations in the soil were measured with a NC Analyzer (NC-22F; SCAS Ltd., Osaka, Japan).

2.5. Statistical analysis

We tested the differences in the soil P fractions among the soil sampling locations at the 0−10 and 10−20 cm soil depths by multiple comparisons assuming unequal distribution among categories (Games-Howell test). The difference in the amount of each soil P fraction between soil depths was tested by Welch's t-test. We investigated the relationship between Al_o, Si_o, Fe_o, Al_p or Fe_p and soil P fractions in the soils at 0−10 and 10−20 cm depths using Spearman's rank correlation (ρ). The relationships between topography (elevation and slope angle) and soil P fractions in the soils at 0–10 and 10–20 cm depths were also analyzed by Spearman's rank correlation.

We applied multiple linear regression models to clarify the factors affecting total Ca-P, Fe-P, and Al-P in the soils from 0−10 and 10−20 cm depths. We used a full model including all possible variables and conducted a stepwise model selection (in both directions) according to Akaike information criterion. The full model for Ca-P includes slope angle, pH, Si_o, Al_p, sum of Ca, Mg, K and Na, and soil depth. The full model for Fe-P and Al-P, which are expected to be strongly related to volcanic ash, includes slope angle, pH, Si_o, Al_p, and soil depth. Before we ran the full model, we ensured that the variance inflation factor for explanatory variables was lower than 10 to avoid multicollinearity. We converted soil depth to binary (0−10 cm and 10−20 cm soil depths were set to 1 and 0, respectively). A significant *p*-value was set as 0.05. Games-Howell tests were performed by an open calculation code provided by Aoki (2009). All statistical analyses were conducted in R version 3.5.3 (R Core Team 2019).

3. Results

3.1. Amount and composition of soil P as determined by the Sekiya method (1970) and soil TP

Regardless of the soil sampling location, the dominant P form was Fe-P, followed by comparable Al-P and Ca-P (Table 3, Tables S2 and S3). The Ca-IP at the 0–10 and 10 –20 cm depths varied from 0 to 203 mg kg^{-1} and there were no clear differences among soil areas (Table S2). Ca-OP at the 0–10cm depth in BFS area was significantly higher than that in the other two areas (Table S3). The Ca-OP was significantly lower than Ca-IP at 0–10 and 10–20 cm soil depths (Table 3). The Al-IP at the 0−10 and 10−20 cm depths varied from 5 to 142 mg kg^{-1} (Table S2). The Al-IP at the 0–10cm depth in BFS area was significantly higher than that in NAA area (Table S3). The Al-OP

was significantly lower than Al-IP at both the 0–10 and 10–20 cm soil depths (Table 3). Al-OP highly varied among the soil sampling points, and most sampling points lack Al-OP fraction (Table S2). Fe-IP at 0−10 and 10−20 cm soil depths ranged from 0 to 251 mg kg^{-1} (Table S2). Fe-OP was equivalent to Fe-IP at both the 0−10 and 10−20 cm soil depths (Table 3).

Soil TP at 0–20 cm soil depth varied from 650 to 2900 mg kg^{-1}, and the soil TP at a depth of 0−20 cm in the igneous rock area was significantly higher than that in the sedimentary rock area (Table S4). The soil TP was significantly correlated with elevation and slope angle and Sekiya TP (ρ = 0.51, 0.61 and 0.83, Table S5).

3.2. Selectively extracted Al, Si and Fe and soil properties

Contrary to our expectation, Al_o, Si_o, and Al_p did not relate with Andosols shown by the soil map. Although $Al_o + 1/2\ Fe_o$ in all soil samples did not exceed 2.0% (Table S1), there were differences in the soil chemical properties among the soil areas (Table 2). Al_o at a depth of 0–10 cm in the BFS area was significantly higher than that from other two soil areas, and the Al_o at the 10–20 cm soil depth had a similar trend. Si_o and $Al_o - Al_p$ in the 0–10 and 10–20 cm soil depths from NAA area were significantly lower than those from the other two areas. Fe_o at both the 0–10 and 10–20 cm soil depths from the AA area were significantly higher than those from the NAA area, and those from the BFS area were between the AA and NAA areas. Al_p at the 0−10 cm soil depth from the NAA and BFS areas were significantly higher than that in the AA area, and the Al_p at the 10−20 cm soil depths had similar trends with those at 0−10 cm depth. Soil pH at the 0−10 and 10−20 cm soil depths from the NAA area were significantly lower than those from other soil areas (Table 2). There was significant positive correlation between soil pH and elevation (Table S6). TC at the

0−10 cm soil depth from the NAA and BFS areas were significantly higher than that at the same depth in the AA area (Table 2). TN at the 0−10 and 10−20 cm soil depths from the NAA and BFS areas tended to be higher than those in the AA area. The relationship between TC or TN and elevation or slope angle were unclear (Table S6).

There were significant correlations between Al_o, Si_o, $Al_o - Al_p$ or Al_p / Al_o, and rising elevation (Table S6). The relationship between Al_o and Si_o, Si_o and $Al_o - Al_p$, or Al_p and Al_p / Al_o, were significantly positive (Table S7). Al_p and Fe_p were significantly correlated with an increase in TC and TN, and Si_o was significantly correlated with a decrease in the TN (Table S8).

3.3. Relationship between soil P determined by Sekiya method and environmental factors

Ca-P, Al-P, Fe-P, TIP, Sekiya TP (sum of Ca-P, Al-P, and Fe-P), and residual P (TP − Sekiya TP) were significantly correlated with elevation and slope angle; however, the relationship between TOP or TIP / Sekiya TP and elevation or slope angle were unclear (Table 4). The correlation between Ca-P and Si_o or $Al_o - Al_p$ was significantly positive (ρ = 0.51 and 0.53), while the correlation between Ca-P and Al_p was significantly negative (ρ = −0.47). Al-P was significantly correlated with Si_o or $Al_o - Al_p$ (ρ = 0.52 and 0.54), while the Al-P and Al_p were significantly negatively correlated (ρ = −0.35; Table 4). Fe-P positively correlated to Si_o and Al_p but not significant, and significantly positively correlated with Al_o and Fe_p (ρ = 0.32 and 0.36; Table 4). The each fraction P, TIP, and Sekiya TP were positively correlated with pH, while the TOP (sum of organic Sekiya P) was not correlated with pH (Table 4). Although the relationship between the Sekiya TP or residual TP and Al_p was insignificant, TIP / Sekiya TP were significantly negatively correlated with the Al_p (Table 4). Ca-IP, Al-IP, Fe-IP, and TIP were negatively correlated with Al_p

273 (Fig. 2, ρ = −0.46, −0.46, −0.06, −0.29), and positively correlated with Si_o (Fig. 3, ρ = 0.52, 0.57,
274 0.18, 0.43). Similarly, the Ca-IP, Al-IP and TIP were negatively correlated with Al_p / Al_o (Fig. S1)
275 and positively correlated with $Al_o - Al_p$ (Table S9).
276 The final multiple linear regression models explained the variations of Ca-P, Al-P, and
277 Fe-P at the 0–10 and 10–20 cm soil depths as 0.24 (R^2_{adj}), 0.34 (R^2_{adj}), and 0.33 (R^2_{adj}), respectively.
278 The model selection for Ca-P showed that Al_p was significant explanatory variable and Si_o, slope
279 angle and soil depth were insignificant variables (Fig. 4). The model selection for Al-P showed
280 that soil depth and slope angle were significant explanatory variables and Si_o and Al_p were
281 remained explanatory variables while they were insignificant (Fig. 4). The positive coefficient of
282 slope angle indicated that a steeper slope resulted in more Al-P. The model selection for Fe-P
283 showed that slope angle, Al_p and soil depth were significant explanatory variables (Fig. 4). Similar
284 to Al-P, a positive coefficient of slope angle indicated that Fe-P increased with an increase in slope
285 angle.
286
287 **4. Discussion**
288 **4.1. Amount and composition of selectively extracted Al, Fe and Si**
289 Al_o (Table 2 and Table S1) was smaller than those in the previous studies in Andosols (e.g., Otani
290 and Ae., 1997; Redel et al., 2016). The small amount of active Al may be caused by several
291 reasons. First, the soil map is rough in the mountainous region in Japan because a thorough
292 investigation of the complex and steep topography is difficult. Second, the mixing of the volcanic
293 ash and bedrock by soil movement occurred (Arai et al., 1984; Imaya et al., 2010a). Third, the
294 various aeolian depositions, such as loess from China and a dry river bed, might decrease the
295 effect of volcanic ash (Inoue and Naruse, 1987; Mizota and Matsushima, 1985).
296 Although the amount of active Al was small, the relationship of Si_o and Al_o was similar

297 to $Al_o - Al_p$ and Al_o (Table S7). The trend supports that Si_o represents allophane and imogolite
298 (Parfitt and Kimble., 1989). However, most $(Al_o - Al_p) / Si_o$ in our sites were larger than 3 (Table
299 S1), while purely allophane and imogolite shows $(Al_o - Al_p) / Si_o$ close to 2 (Parfitt and Henmi,
300 1982). Excess Al might come from Al substituted in ferrihydrite and hydroxy Al in the interlayer
301 of 2 : 1 and 2 : 1 : 1 layer silicate intergrades (Dahlgren and Ugolini, 1991; Shoji and Fujiwara,
302 1984). There was a significant inverse relationship between Si_o and Al_p (Table S7), similar to
303 Andosols in a mountainous region (e.g., Takahashi and Shoji, 1996). The inverse relationship
304 between Si_o and Al_p was consistent with the inhibition of allophane and imogolite production by
305 the formation of Al-humus complexes (Takahashi and Dahlgren, 2016).
306
307 **4.2. Soil P fraction by the Sekiya method and soil TP across sampling area**
308 The dominant P form was Fe-P regardless of the location of the soil sample (Table S2). The higher
309 Fe-P compared with Al-P was similar to the trends observed in non-volcanic forest soils (Barosso
310 and Nahas, 2005; Yang et al., 2010), not to those observed in volcanic soils (Nakamura et al.,
311 2019; Otani and Ae, 1997; Tani et al., 2010).
312 Soil TP in soils on igneous rock area was significantly higher than that on sedimentary
313 rock area (Table S4). This pattern was consistent to the report in Dieter et al. (2010) that higher
314 soil TP content in andesite sites than marine sediment sites in Panama. However, we found a
315 significant relationship between soil TP and elevation as well as between lithologies (Table S5).
316 The elevation correlated with Ca, Mg, K, and Na (Table S10) and sum of them (Fig. S2) while
317 the relationship between these elements and the lithology were unclear. Kitayama et al. (2000)
318 discussed that the changes in primary P in the soil along the altitudinal gradient may relate to the
319 rock weathering on sedimentary rock. We found a significant positive correlation between sum of
320 Ca, Mg, K, and Na and soil TP in both lithologies (Fig. S3). Thus, the variation of soil TP across

sites may relate to the rock weathering as well as difference of the lithologies. The significant correlation between Ca-P, Fe-P, Al-P, and Sekiya TP with elevation (Table 4), and also that between elevation and Al_o, Si_o, pH, soil TP (Table S5 and S6) suggested that Ca-P, Fe-P, Al-P, and Sekiya TP were strongly affected by the gradient of soil P stock. The initial amount of volcanic material that was deposited in the watershed was unknown, but the variation caused by the complex topography might result in the observed distribution of Si_o or Al_o.

4.3. Effect of topography and active Al on Fe-P and Al-P

Multiple regression models for Al-P and Fe-P showed that slope angle and Al_p were significant explanatory variables (Fig. 4). These results suggest that topography and active Al were equally important in determining distribution of soil P fraction. A few studies have shown that larger NaOH extracted P in valleys or lower slopes compared with that observed on the ridge or upper slopes (Mage and Porder, 2013; Vitousek et al., 2003) may be caused by soil deposition from the upper slope (Mage and Porder, 2013). Slope angle can represent the soil accumulated from the upper slope on the small headwater catchment since we collected soil samples from the foot of the slope. The degree of soil erosion and deposition is different by slope angle and vegetation (Wakiyama et al., 2001) and further research is needed to clarify the effect of slope angle on soil P fraction.

The regression analysis indicates that Al_p contributes to Fe-P accumulation at our site (Fig. 4), suggesting that Al-humus complexes increased Fe-P. We operationally defined Fe-P in NaOH extract and such alkaline solution also extracts humus (Ohno et al., 2019). Thus, it is reasonable that Fe-P in organic form, which dominated half of the fraction (Table 3) came from humus. The positive correlations between Fe-P with TC and TN, between Al_p and TC or TN (Table S8), and between Fe_p and Fe-OP (Table S9) support this idea. Soil humus contains amorphous Al

345 as well as Fe (Vincent et al., 2012), so Al-associated P as well as Fe-associated P are present in
346 the Fe-P fraction.

347 Al-P significantly increased with Si_o ($\rho = 0.52$, Table 4) which indicates that amorphous
348 minerals increased Al-associated P. However, the correlation between Al-P and Al_p was
349 significantly negative ($\rho = -0.35$, Table 4). In addition, multiple regression models showed that
350 the coefficients of Si_o and Al_p were positive and negative, respectively. These results suggest that
351 effects of allophane and imogolite, and Al-humus complexes are different. The effect of Al_p on
352 Al-P was negative and suggests that the accumulation mechanism is different for Al-P than for
353 Fe-P. In contrast to Fe-P, Al-P mainly consisted of the inorganic form (Table 3), since the neutral
354 NH_4F solution extracts little soil P in organic form. NH_4F is considered to extract P associated
355 with aluminosilicate including allophane (Chang and Jackson, 1957; Sekiya, 1970). We observed
356 a negative relationship between Al-IP and Al_p (Fig. 2) suggesting that Al-humus complexes can
357 decrease microbial P mineralization (Redel et al., 2016). It is well known that Al and Fe oxides
358 contribute to the accumulation of organic P in temperate and non-volcanic soils (Stutter et al.,
359 2015; Zederer and Talkner 2018). Laboratory experiments confirmed that Al and Fe ions sorb
360 organic P, such as inositol and humus, and prevent these organic P from microbial degradation
361 (Givano et al. 2010; Schneider et al., 2010; Tang et al., 2006). Therefore, P that is
362 absorbed/adsorbed to Al_p can keep P in organic form from microbial mineralization. In addition,
363 some studies reported that negative relationships between KCl-extracted Al and soil enzyme
364 activity, microbial respiration, and microbial biomass (Illmer et al., 2003; Kunito et al., 2016).
365 These negative relationships are caused by Al toxicity for microbes (Illmer et al. 1995). When the
366 P fraction mainly consisted of the inorganic form, negative effect of Al_p may appear, as analogous
367 to the role of Al_p on a lower rate of soil C decomposition (Rasmussen et al., 2006) at the same
368 time it contributes to the accumulation of total soil carbon (Imaya et al., 2010b).

4.4. Effect of active Al on Ca-P and inorganic P

Ca-P that indicates available P in the Sekiya method (Sekiya, 1970) was explained by negative effect of Al_p and positive effect of Si_o in the multiple regression analysis (Fig. 4). Further, the correlation between Ca-P and $Al_o - Al_p$ or Al_p / Al_o were significantly positive and negative, respectively (Table 4). Previous studies reported that negative or unclear effects of allophane or $Al_o - Al_p$ on the amount of available P (Redel et al., 2016; Satti et al., 2007). Available P is a rapid turnover fraction and a portion of their sources is phytate salt. Tang et al. (2006) found that the coexistence of Fe or Al ions with Ca ion hampered phytase activity. This is because precipitates of phytate and Fe or Al ions is more stable than that of phytate and Ca ion (Maenz et al., 1999; Zhu et al., 2015). The positive relationship between Si_o and Ca-P (Table 4) appears inconsistent with these findings since Si_o represents allophane and imogolite.

The inverse coeffects of Si_o and Al_p on inorganic P were also found in Al-IP and TIP (Figs. 2 and 3), as well as on the ratio of TIP to Sekiya TP (Table 4). In addition, there were significant negative relationships between Al_p / Al_o and Ca-IP, Al-IP, and TIP (Table 4 and Fig. S1). These results suggest that the composition of active Al affected inorganic soil P dynamics. Non-allophanic Andosols, which are characterized by abundant Al-humus complexes and larger Al_p / Al_o, have stronger Al toxicity to some soil microbes than allophanic Andosols (Furuya et al., 1999; Mizuno et al., 1998). The stronger Al toxicity may relate to acidic (pH (H_2O) < 5) conditions, that produce excess Al-humus complexes (Shoji and Fujiwara, 1984). In addition, non-allophanic Andosols can release more Al ions than allophanic Andosols, since Al-humus complexes more weakly hold the Al ions compared with allophane and imogolite (Dahlgren and Saigusa, 1994). The lower elevation sites where observed pH (H_2O) < 5 (Table 1 and Table S2), lower Al_o (Table S6), and moderate Al_p (Table S1), Al toxicity dissolved from Al_p possibly inhibit P mineralization

by microbes. It is necessary to clarify the effect of Al-humus complexes and the composition of active Al on microbial activity and soil P dynamics in soils under the influence of volcanic materials.

5. Conclusion

We investigated the relationship between the two types of active Al (amorphous minerals and Al-humus complexes) and sequentially extracted soil P in soils from Japanese cedar forests in a watershed. Regardless of the sampling point, the Al_o concentration was low, and the dominant P form was Fe-P followed by Al-P and Ca-P. Fe-P consisted of comparable organic and inorganic forms, while Al-P and Ca-P were dominated by inorganic forms. Although the concentration of active Al was low, it significantly correlated with soil P forms, and the trend was different with different types of active Al. Specifically, Al-P was significantly positively correlated with Si_o but significantly negatively correlated with Al_p. Contrast to this, Fe-P was positively correlated with Al_p. The multiple regression models showed that Ca-P, Al-P and Fe-P were explained by Si_o and Al_p as well as topographic and geographic factors. Fe-P was explained by positive effects of slope angle and Al_p, suggesting that Fe-P was increased by an accumulation of soil and humus complex with Al on the steeper slope. Contrary to this, Ca-P and Al-P was explained by positive effect of the slope angle and Si_o and negative effect of Al_p. These results suggested that Al_p possibly inhibited P mineralization by microbes. Our results indicated that the two types of active Al have different effects on the soil P forms and may result in the distinctive P dynamics in forest ecosystems.

Acknowledgements

This study was supported by JSPS KAKENHI (19K15873). We thank the members of the ecosystem management laboratory in Akita Prefectural University for assistance with field work and chemical analyses. We thank Tara Penner, MSc, from Edanz Group (https://en-author-services.edanz.com/ac) for editing a draft of this manuscript.

References

Achat, D. L., Augusto, L., Gallet-Budynek, A., Bakker, M. R. 2012. Drying-induced changes in phosphorus status of soils with contrasting soil organic matter contents – Implications for laboratory approaches. Geoderma 187–188, 41-48. https://doi.org/10.1016/j.geoderma.2012.04.014.

Aoki, S., 2009. Tukey's multiple comparisons. http://aoki2.si.gunma-u.ac.jp/R/tukey.html (Last modified Aug 03, 2009)

Arai, S., Oshima, T., Kumada, K. 1984. Volcanic glass of forest soils in north-eastern Aichi. Pedologist 28, 98–107. (Japanese with English summary) https://doi.org/10.18920/pedologist.28.2_98

Barroso, C.B., Nahas, E., 2005. The status of soil phosphate fractions and the ability of fungi to dissolve hardly soluble phosphates. Appl. Soil Ecol. 29, 73–83. doi:10.1016/j.apsoil.2004.09.005

Barrow, N.J., Sen, A., Roy, N. Debnath, A. 2021. The soil phosphate fractionation fallacy. Plant Soil 459, 1–11. https://doi.org/10.1007/s11104-020-04476-6

Borie, F., Rubio, R., 2003. Total and organic phosphorus in Chilean volcanic soils. Gayana Bot. 60, 69–78.

Brady, N.C., Weil, R.R., 2003. The nature and properties of soils. 14th edition, Pearson Education, Inc.

Chang, S.C., Jackson, M.L. 1957. Fractionation of soil phosphorus. Soil Sci. 84, 133–144.

Comfort, S.D., Dick, R.P., Baham, J. 1991. Air-Drying and Pretreatment Effects on Soil Sulfate

441 Sorption. Soil Sci. Soc. America J. 55, 968–973.
442 https://doi.org/10.2136/sssaj1991.03615995005500040012x
443 Cornelis, JT., Titeux, H., Ranger, J., Delvaux, B. 2011. Identification and distribution of the readily
444 soluble silicon pool in a temperate forest soil below three distinct tree species. Plant Soil 342,
445 369–378. https://doi.org/10.1007/s11104-010-0702-x
446 Crews, T.E., Kitayama, K., Fownes, J.H., Riley, R.H., Herbert, D.A., Mueller-Dombois, D., Vitousek,
447 P.M. 1995. Changes in Soil Phosphorus Fractions and Ecosystem Dynamics across a Long
448 Chronosequence in Hawaii. Ecology 76, 1407–1424.
449 Dahlgren, R.A., Saigusa, M., 1994. Aluminum release rates from allophanic and nonallophanic
450 Andosols. Soil Sci.Plant Nutr., 40, 125–136. https://doi.org/10.1080/00380768.1994.10414285
451 Dahlgren, R.A., Ugolini, F.C., 1991. Distribution and characterization of short-range-order minerals
452 in spodosols from the Washington cascades. Geoderma, 48, 391–413.
453 https://doi.org/10.1016/0016-7061(91)90056-Y.
454 Dieter, D., Elsenbeer, H., Turner, BL., 2010. Phosphorus fractionation in lowland tropical rainforest
455 soils in central Panama. CATENA, 82, 118–125. https://doi.org/10.1016/j.catena.2010.05.010.
456 Elser, J.J., Bracken, M.E.S., Cleland, E.E., Gruner, D.S., Harpole, W. S., Hillebrand, H., Ngai, J.T.,
457 Seabloom, E.W., Shurin, J.B., Smith, J.E. 2007. Global analysis of nitrogen and phosphorus
458 limitation of primary producers in freshwater, marine and terrestrial ecosystems. Ecol. Lett.,10,
459 1135–1142. doi: 10.1111/j.1461-0248.2007.01113.x
460 Furuya, H., Takahashi, T., Matsumoto, T., 1999. Suppression of Fusarium Solani F. Sp. Phaseoli on
461 Bean by Aluminum in Acid Soils. Phytopathology 89, 47–52. doi: 10.1094/PHYTO.1999.89.1.47.
462 Giaveno, C., Celi, L., Richardson, A.E., Simpson, R.J., Barberis. 2010. Interaction of phytases with
463 minerals and availability of substrate affect the hydrolysis of inositol phosphates, Soil Biol
464 Biochem 42, 491–498. https://doi.org/10.1016/j.soilbio.2009.12.002.

Gu, C., Wilson, G.S., Margenot, J.A., 2020. Lithological and bioclimatic impacts on soil phosphatase activities in California temperate forests, Soil Biol. Biochem., 141, 107633, https://doi.org/10.1016/j.soilbio.2019.107633.

Hayakawa, A., Funaki, Y., Sudo, T., Asano, R., Murano, H., Watanabe, S., Ishida, T., Ishikawa, Y., Hidaka, S., 2020. Catchment topography and the distribution of electron donors for denitrification control the nitrate concentration in headwater streams of the Lake Hachiro watershed, Soil Sci. Plant Nutr. 66, 906-918, DOI: 10.1080/00380768.2020.1827292

Hedley, M.J., Stewart, J.W.B., Chauhan, B.S., 1982. Changes in inorganic and organic soil phosphorus fractions induced by cultivation practices and laboratory incubation. Soil Sci. Soc. Am. J. 46, 970–976.

Illmer, P., Marschall, K. and Schinner, F., 1995. Influence of available aluminium on soil micro-organisms. Lett Appl Microbiol 21: 393–397. https://doi.org/10.1111/j.1472-765X.1995.tb01090.x

Illmer, P., Obertegger, U., Schinner, F. 2003. Microbiological Properties in Acidic Forest Soils with Special Consideration of KCl Extractable Al. Water, Air, & Soil Pollution 148, 3–14. https://doi.org/10.1023/A:1025422229468

Imaya, A., Ohta, S., Tanaka, N. and Inagaki, Y., 2005. General Chemical Properties of Brown Forest Soils Developed from Different Parent Materials in the Submontane Zone of the Kanto and Chubu Districts, Japan. Soil Sci. Plant Nutr. 51, 873–884. DOI: 10.1111/j.1747-0765.2005.tb00122.x

Imaya, A., Yoshinaga, S., Inagaki, Y., Tanaka, N., Ohta, S. 2010a. Proposal for advanced classification of brown forest soils in Japan with reference to the degree of volcanic ash additions, Soil Sci. Plant Nutr. 56, 454–465. DOI: 10.1111/j.1747-0765.2010.00464.x

Imaya, A., Yoshinaga, S., Inagaki, Y., Tanaka, N., Ohta, S., 2010b. Volcanic ash additions control soil

carbon accumulation in brown forest soils in Japan, Soil Sci. Plant Nutr. 56, 734–744, DOI: 10.1111/j.1747-0765.2010.00508.x

Inoue, K., Naruse, T., 1987. Physical, Chemical, and Mineralogical Characteristics of Modern Eolian Dust in Japan and Rate of Dust Deposition, Soil Sci. Plant Nutr., 33, 327–345, DOI: 10.1080/00380768.1987.10557579

Kitayama, K., Majalap-Lee, N., Aiba, S. 2000. Soil phosphorus fractionation and phosphorus-use efficiencies of tropical rainforests along altitudinal gradients of Mount Kinabalu, Borneo. Oecologia 123, 342–349. https://doi.org/10.1007/s004420051020

Kruse, J., Abraham, M., Amelung, W., Baum, C., Bol, R., Kühn, O., Lewandowski, H., Niederberger, J., Oelmann, Y., Rüger, C., Santner, J., Siebers, M., Siebers, N., Spohn, M., Vestergren, J., Vogts, A. and Leinweber, P. 2015. Innovative methods in soil phosphorus research: A review. J. Plant Nutr. Soil Sci., 178: 43-88. https://doi.org/10.1002/jpln.201400327

Kunito, T., Isomura, I., Sumi, H., Park, H., Toda, H., Otsuka, S., Nagaoka, K., Saeki, K., Senoo, K., 2016. Aluminum and acidity suppress microbial activity and biomass in acidic forest soils. Soil Biol. Biochem. 97, 23–30.

Kuo, S., 1996. Phosphorus. *In* Methods of soil analysis. Agronomy 9, Ed. Sparks DL, ASA-SSA, Madison, Wisconsin, USA.

Maenz, D.D., Engele-Schaan, M. C., Newkirk, W. R., Classen, L. H., 1999. The effect of minerals and mineral chelators on the formation of phytase-resistant and phytase-susceptible forms of phytic acid in solution and in a slurry of canola meal, Anim Feed Sci Tech 81, 177–192. https://doi.org/10.1016/S0377-8401(99)00085-1.

Mage, S.M., Porder, S., 2013. Parent Material and Topography Determine Soil Phosphorus Status in the Luquillo Mountains of Puerto Rico. Ecosystems 16, 284–294. https://doi.org/10.1007/s10021-012-9612-5

513 Matsuyama, N., Kudo, K., Saigusa, M., 1999. Active aluminum of cultivated Andosols and related
514 soil chemical properties in Japan. Bull. Fac. Agric. Life Sci. Hirosaki Univ. 1, 30–36.
515 Mikutta, R., Kleber, M., Torn, M.S., Jahn, R., 2006. Stabilization of Soil Organic Matter: Association
516 with Minerals or Chemical Recalcitrance? Biogeochemistry 77, 25–56.
517 https://doi.org/10.1007/s10533-005-0712-6
518 Mizota, C., Matsuhisa, Y., 1985. Eolian Additions to Soils and Sediments of Japan, Soil Sci. Plant Nutr.
519 31, 369–382, DOI: 10.1080/00380768.1985.10557444
520 Mizuno, N., Yoshida, H., Nanzyo, M., Tadano, T., 1998. Chemical characterization of conducive and
521 suppressive soils for potato scab in Hokkaido, Japan. Soil Sci. Plant Nutr. 44, 289–295. DOI:
522 10.1080/00380768.1998.10414451
523 Mukai, M., Aiba, S., Kitayama, K., 2016. Soil-nutrient availability and the nutrient-use efficiencies of
524 forests along an altitudinal gradient on Yakushima Island, Japan. Ecol. Res. 31, 719–730. DOI
525 10.1007/s11284-016-1381-8
526 Nakamura, Y., Ando K., Tsunekawa, A., Kasuya, M., 2019. Effects of continuous use of livestock
527 manure on phosphorus leaching and phosphorus forms in sandy upland field. Jpn. J. Soil Sci.
528 Plant Nutr. 90, 212–216. (Japanese)
529 Newman, E.I., 1995. Phosphorus inputs to terrestrial ecosystems. J. Ecology 83, 713–726.
530 Obara, H., Ohkura, T., Takata, Y., Kohyama, K., Maejima, Y., Hamazaki, T., 2011. Comprehensive
531 Soil Classification System of Japan. Bull. National institute for agro-environmental sciences 29,
532 1−73.
533 Ohno, T., Hess, N.J., Qafoku, N.P. 2019. Current Understanding of the Use of Alkaline Extractions of
534 Soils to Investigate Soil Organic Matter and Environmental Processes. J. Environ. Qual. 48,
535 1561–1564. doi:10.2134/jeq2019.08.0292
536 Otani, T., Ae, N., 1997. The status of inorganic and organic phosphorus in some soils in relation to

plant availability. Soil Sci. Plant Nutr. 43, 419–429. doi: 10.1080/00380768.1997.10414765

Parfitt, R.L. and Kimble, J.M. 1989. Conditions for Formation of Allophane in Soils. Soil Sci. Soc. America J. 53, 971–977. https://doi.org/10.2136/sssaj1989.03615995005300030057x

Parfitt, R.L. and Henmi, T. 1982. Comparison of an oxalate-extraction method and an infrared spectroscopic method for determining allophane in soil clays, Soil Sci. Plant Nutr., 28, 183-190. https://doi.org/10.1080/00380768.1982.10432435

Porder, S., Paytan, A., Vitousek, P.M., 2005. Erosion and landscape development affect plant nutrient status in the Hawaiian Islands. Oecologia 142**,** 440–449. https://doi.org/10.1007/s00442-004-1743-8

Porder, S., Ramachandran, S. 2013. The phosphorus concentration of common rocks—a potential driver of ecosystem P status. Plant Soil 367, 41–55. DOI 10.1007/s11104-012-1490-2

Rasmussen, C., Southard, R.J., Horwath, W.R. 2006. Mineral control of organic carbon mineralization in a range of temperate conifer forest soils. Global Change Biol. 12: 834-847. https://doi.org/10.1111/j.1365-2486.2006.01132.x

R Core Team, 2019. R: A language and environment for statistical computing. R Foundation for Statistical Computing, Vienna, Austria. URL https://www.R-project.org/.

Redel, Y., Rubio, R., Godoy, R., Borie, F., 2008. Phosphorus fractions and phosphatase activity in an Andisol under different forest ecosystems. Geoderma 145, 216–221. doi:10.1016/j.geoderma.2008.03.007

Redel, Y., Cartes, P., Demanet, R., Velásquez, G., Poblete-Grant, P., Bol, R., Mora, M.L., 2016. Assessment of phosphorus status influenced by Al and Fe compounds in volcanic grassland soils. J. Soil Sci. Plant Nutr. 16, 490–506.

Saigusa, M., Matsuyama, N., Honna, T., Abe, T., 1991. Chemistry and fertility of acid Andisols with special reference to subsoil acidity. In: Wright, R.J., Baligar, V.C., Murrmann, R.P. (Eds.),

561 Plant–Soil Interactions At Low pH. Developments in Plant and Soil Sciences. Springer,
562 Netherlands, pp. 73–80.
563 Satti, P., Mazzarino, M.J., Roselli., Crego, P., 2007. Factors affecting soil P dynamics in temperate
564 volcanic soils of southern Argentina. Geoderma 139, 229–240.
565 Sekiya, K., 1970. Phosphorus. *In* Methods of soil analysis (Dojyou youbun bunsekihou), Ed.
566 Ministry of agriculture, forestry and fisheries, Youkendou, Tokyo. (In japanese)
567 Schlesinger, W.H., Bruijnzeel, L.A., Bush, M.B., Klein, E.M., Mace, K.A., Raikes, J.A., Whittaker,
568 R.J., 1998. The biogeochemistry of phosphorus after the first century of soil development on
569 Rakata Island, Krakatau, Indonesia. Biogeochemistry 40, 37–55.
570 https://doi.org/10.1023/A:1005838929706
571 Schneider, M. P. W., Scheel, T., Mikutta, R., van Hees, P., Kaiser, K., Kalbitz, K. 2010. Sorptive
572 stabilization of organic matter by amorphous Al hydroxide. Geochim Cosmochim Ac 74, 1606–
573 619. https://doi.org/10.1016/j.gca.2009.12.017
574 Sharpley A.N., Tiessen, H., Cole, C.V., 1987. Soil phosphorus forms extracted by soil tests as a
575 function of pedogenesis. Soil Sci. Soc. Am. J. 41, 362–365.
576 Shoji, S., Fujiwara, Y., 1984. Active aluminum and iron in the humus horizons of Andosols from
577 northeastern Japan: Their forms, properties, and significance in clay weathering. Soil Sci. 137,
578 216–226.
579 Shoji, S., Nanzyo, M., Dahlgren, R.A., 1993. Volcanic Ash Soils — Genesis, Properties and
580 Utilization. Elsevier, Amsterdam.
581 Stahr, S., Graf-Rosenfellner, M., Klysubun, W., Mikutta, R., Prietzel, J., Lang, F. 2018. Phosphorus
582 speciation and C:N:P stoichiometry of functional organic matter fractions in temperate forest soils.
583 Plant Soil 427, 53–69. https://doi.org/10.1007/s11104-017-3394-7
584 Stutter, M.I., Shand, C.A., George, T.S., Blackwell, M S.A., Dixon, L., Bol, R., MacKay R.L.,

585 Richardson, A.E., Condron, L.M., Haygarth, P.M. 2015. Land use and soil factors affecting
586 accumulation of phosphorus species in temperate soils, Geoderma 257–258, 29–39.
587 https://doi.org/10.1016/j.geoderma.2015.03.020.
588 Takahashi, T., Dahlgren, R.A., 2016. Nature, properties and function of aluminum–humus complexes
589 in volcanic soils. Geoderma 263, 110−121. http://dx.doi.org/10.1016/j.geoderma.2015.08.032
590 Takahashi, T., Shoji, S., 1996. Active aluminum status in surface horizons showing continuous
591 climosequence of volcanic ash-derived soils in Towada district, northeastern Japan, Soil Sci.
592 Plant Nutr., 42, 113–120, DOI: 10.1080/00380768.1996.10414694
593 Tani, M., Mizota, C., Yagi, T., Kato, T. and Koike, M., 2010. Vertical distribution and accumulation of
594 phosphate in virgin soils and arable soils of Tokachi district, Hokkaido. Jpn J. Soil Sci. Plant Nutr.
595 81, 350−359. (Japanese with English summary)
596 Tang, J., Leung, A., Leung, C., Lim, L.B., 2006, Hydrolysis of precipitated phytate by three distinct
597 families of phytases, Soil Biol Biochem 38, 1316–1324.
598 https://doi.org/10.1016/j.soilbio.2005.08.021.
599 Torii, A. 1990. Mode of deposition inferred from tephra-origin particles included in granite soils in
600 Kinki and Sanyo mountain areas. Pedologist 34, 104−118. (Japanese with English summary)
601 https://doi.org/10.18920/pedologist.34.2_104
602 Tsai, C.C., Chen, Z.S., Kao, C.I., Ottner, F., Kao, S.J., Zehetner, F., 2010. Pedogenic development of
603 volcanic ash soils along a climosequence in Northern Taiwan. Geoderma 156, 48 − 59.
604 https://doi.org/10.1016/j.geoderma.2010.01.007.
605 Vincent, A.G., Schleucher, J., Gröbner, G., Vestergren, j., Persson, P., Jansson, M., Giesler, R. 2012.
606 Changes in organic phosphorus composition in boreal forest humus soils: the role of iron and
607 aluminium. Biogeochemistry 108, 485–499. https://doi.org/10.1007/s10533-011-9612-0
608 Vitousek, P., Chadwick,O., Matson, P., Allison, S., Derry, L., Kettley, L., Luers, A., Mecking, E.,

609 Monastra, V., Porder, S., 2003. Erosion and the rejuvenation of weathering-derived nutrient
610 supply in an old tropical landscape. Ecosystems 6, 762–772. DOI: 10.1007/s10021-003-0199-8
611 Vitousek, P.M., Porder, S., Houlton, B.Z. and Chadwick, O.A. 2010. Terrestrial phosphorus limitation:
612 mechanisms, implications, and nitrogen–phosphorus interactions. Ecol. App. 20, 5–15.
613 doi:10.1890/08-0127.1
614 Walker, T.W., Syers, J.K., 1976. The fate of phosphorus during pedogenesis. Geoderma 15,1−19
615 WRB 2014. World reference base for soil resources 2014.
616 Yang, K., Zhu,J., Yan, Q., Sun, O.J., 2010. Changes in soil P chemistry as affected by conversion of
617 natural secondary forests to larch plantations. For. Ecol. Manage. 260, 422–428.
618 doi:10.1016/j.foreco.2010.04.038
619 Zederer, D.P., Talkner., 2018, Organic P in temperate forest mineral soils as affected by humus form
620 and mineralogical characteristics and its relationship to the foliar P content of European beech,
621 Geoderma 325, 162–171. https://doi.org/10.1016/j.geoderma.2018.03.033.
622 Zhu, Y., Wu, F., He, Z., Giesy, P.J., Feng, W., Mu, Y., Feng, C., Zhao, X., Liao, H., Tang, Z., 2015.
623 Influence of natural organic matter on the bioavailability and preservation of organic phosphorus
624 in lake sediments, Chemical Geology 397, 51–60.
625 https://doi.org/10.1016/j.chemgeo.2015.01.006.
626

627

628 **Figure captions**

629

630 **Fig. 1 Map of the Hachiro-gata watershed. The central land is Hachiro-gata polder,**
631 **surrounded by relict lake. Light blue lines indicate flowing rivers flowing into**
632 **the lake. Yellow points indicate soil sampling points. Blue, red, and brown shaded**
633 **land represent areas of NAA (non-allophanic Andosols), AA (allophanic**
634 **Andosols), and BFS (Brown forest soils), respectively.**

635

636 **Fig. 2 Relationship between Ca-P, Al-P, Fe-P, TIP, and Al_p at soil depths of 0–10 cm**
637 **and 10–20 cm. Asterisks indicate significant correlations ($p < 0.05$).**

638

639 **Fig. 3 Relationship between Ca-P, Al-P, Fe-P, TIP, and Si_o at soil depths of 0–10 cm**
640 **and 10–20 cm. Asterisks indicate significant correlations ($p < 0.05$).**

641

642 **Fig. 4 Standardized coefficients of the finally selected multiple linear regression**
643 **models. Values represent standardized coefficients, and the error of the**
644 **explanatory variables. Al_p: pyrophosphate-extracted Al; slope angle: median of**
645 **the slope in the headwater catchment. Positive coefficient of soil depth indicates**
646 **that the response variable was larger at the shallower depth. Asterisks indicate**
647 **significant coefficients ($p < 0.05$).**

648

649

Table 1 Site characteristics of soil sampling points

ID	Soil area	Lithological area	Catchment area (km^2)	Elevation (m)	Slope angle (°)
1	NAA	Sedimentary	0.83	80	15
3	NAA	Sedimentary	1.88	104	22
4	NAA	Sedimentary	1.98	106	22
5	NAA	Sedimentary	1.17	106	22
6	NAA	Sedimentary	2.38	186	22
8	NAA	Sedimentary	6.75	197	26
9	NAA	Sedimentary	3.46	198	23
10	NAA	Sedimentary	1.93	147	22
11	NAA	Sedimentary	0.98	151	26
12	AA	Sedimentary	1.54	147	25
13	AA	Sedimentary	2.21	122	24
14	AA	Igneous	4.69	205	29
15	AA	Sedimentary	1.61	135	24
16	AA	Sedimentary	2.32	156	30
17	AA	Sedimentary	1.82	152	31
18	AA	Sedimentary	1.30	150	27
19	AA	Sedimentary	0.75	162	30
20	AA	Sedimentary	0.55	114	28
21	AA	Sedimentary	3.29	220	27
22	AA	Sedimentary	2.55	162	26
23	AA	Sedimentary	3.30	215	24
25	BFS	Igneous	12.12	451	32
26	BFS	Sedimentary	16.89	388	31
28	BFS	Sedimentary	1.87	294	32
29	BFS	Igneous	5.08	297	27
30	BFS	Sedimentary	1.26	165	22
31	BFS	Igneous	3.80	447	31
32	BFS	Igneous	1.87	294	32
33	BFS	Igneous	1.69	331	34

NAA: non-allophanic Andosols, AA: allophanic Andosols, BFS: Brown forest soils

650

Table 2 Chemical properties in soils from 0–10 cm and 10–20 cm depths in the different soil areas

	(cm)		(g kg^{-1})	(g kg^{-1})	(g kg^{-1})	(g kg^{-1})	(g kg^{-1})	(g kg^{-1})	(%)	(%)
Soil area	depth	pH (H_2O)	Al_o	Fe_o	Si_o	Al_p	Fe_p	$Al_o - Al_p$	TC	TN
NAA	0-10	4.8 ± 0.3a	3.1 ± 0.8a	6.0 ± 1.7a	0.23 ± 0.07a	2.4 ± 0.8b	3.4 ± 1.5ab	0.69 ± 0.25a	4.6 ± 1.3b	0.32 ± 0.10
	10-20	4.8 ± 0.3a	3.3 ± 1.0a	5.7 ± 2.0a	0.21 ± 0.05a	2.8 ± 1.3ab	3.5 ± 2.0	0.45 ± 0.53a	2.6 ± 1.1	0.22 ± 0.07
AA	0-10	5.6 ± 0.4b	3.9 ± 1.1a	8.3 ± 2.3b	0.61 ± 0.30b	1.6 ± 0.7a	2.1 ± 0.7a	2.31 ± 1.19b	3.3 ± 1.2a	0.22 ± 0.08
	10-20	5.5 ± 0.4b	3.9 ± 1.2ab	8.5 ± 1.8b	0.54 ± 0.27b	1.8 ± 0.8a	2.3 ± 0.6	2.13 ± 1.30b	1.9 ± 0.6	0.15 ± 0.04
BFS	0-10	5.3 ± 0.3b	6.3 ± 2.3b	7.6 ± 2.3ab	0.66 ± 0.24b	3.2 ± 1.2b	3.2 ± 0.8b	3.07 ± 1.84b	4.8 ± 1.4b	0.31 ± 0.10
	10-20	5.3 ± 0.3b	5.9 ± 2.1b	7.1 ± 1.9ab	0.66 ± 0.24b	3.4 ± 1.4b	3.3 ± 0.9	2.54 ± 1.60b	2.7 ± 1.5	0.21 ± 0.11

NAA: non-allophanic Andosols, AA: allophanic Andosols, BFS: Brown forest soils, Al_o: oxalate-extracted aluminum, Fe_o: oxalate-extracted iron, Si_o: oxalate-extracted silicate, Al_p: pyrophosphate-extracted aluminum, Fe_p: pyrophosphate-extracted iron, TC: total carbon, TN: total nitrogen. Lower case letters indicate significant differences among soil areas at each soil depth by multiple comparisons (Games-Howell test).

Table 3 Sekiya P (mgP kg^{-1}) at 0–10 cm and 10–20 cm soil depths

Fraction	0-10 cm	10–20 cm
Ca-IP	40 ± 46b	23 ± 33b
Ca-OP	2.4 ± 3.7a	1.3 ± 1.5a
Al-IP*	57 ± 41b	33 ± 28b
Al-OP	4.8 ± 13a	2.6 ± 9.9a
Fe-IP*	151 ± 41c	82 ± 54c
Fe-OP	112 ± 87c	128 ± 79c

Values represent means ± the standard deviations of the mean (n = 29). IP: inorganic phosphorus, OP: organic phosphorus. Lower case letters indicate significant differences among the fractions within each soil depth by multiple comparisons (Games-Howell test, $p < 0.05$). Asterisks indicate significant differences between the soil depths in each fraction by Welch's t-test ($p < 0.05$).

Table 4 Spearman's correlation (ρ) of soil P with environmental varieties at the 0–10 cm and 10–20 cm soil depths

	Elevation	Slope angle	Soil TP	Al_o	Si_o	Fe_o	Al_p	Fe_p	$Al_o - Al_p$	Al_p / Al_o	pH
Ca-P	0.39*	0.43*	0.57*	0.09	0.51*	0.21	−0.47*	−0.41*	0.53*	−0.63*	0.45*
Al-P	0.49*	0.48*	0.63*	0.19	0.52*	0.22	−0.35*	−0.31*	0.54*	−0.57*	0.48*
Fe-P	0.28*	0.32*	0.47*	0.32*	0.22	0.17	0.17	0.36*	0.24	−0.08	0.05
TIP	0.41*	0.39*	0.55*	0.17	0.43*	0.16	−0.29*	−0.25	0.47*	−0.50*	0.34*
TOP	0.19	0.20	0.32*	0.25	0.05	0.06	0.26	0.45*	0.06	0.10	−0.01
Sekiya TP	0.44*	0.41*	0.64*	0.30*	0.42*	0.21	−0.08	0.06	0.42*	−0.35*	0.29*
Residual P	0.27*	0.37*	0.85*	0.21	0.39*	0.34*	−0.21	−0.17	0.40*	−0.45*	0.33*
TIP / Sekiya TP	0.07	0.02	0.03	−0.06	0.20	0.10	−0.31*	−0.43*	0.20	−0.32*	0.15

TIP: total inorganic P, TOP: total organic P, Sekiya TP: sum of Ca-P, Al-P, and Fe-P, Residual P = TP − Sekiya TP. Asterisks indicate significant correlations between components ($p < 0.05$).

Fig. 1

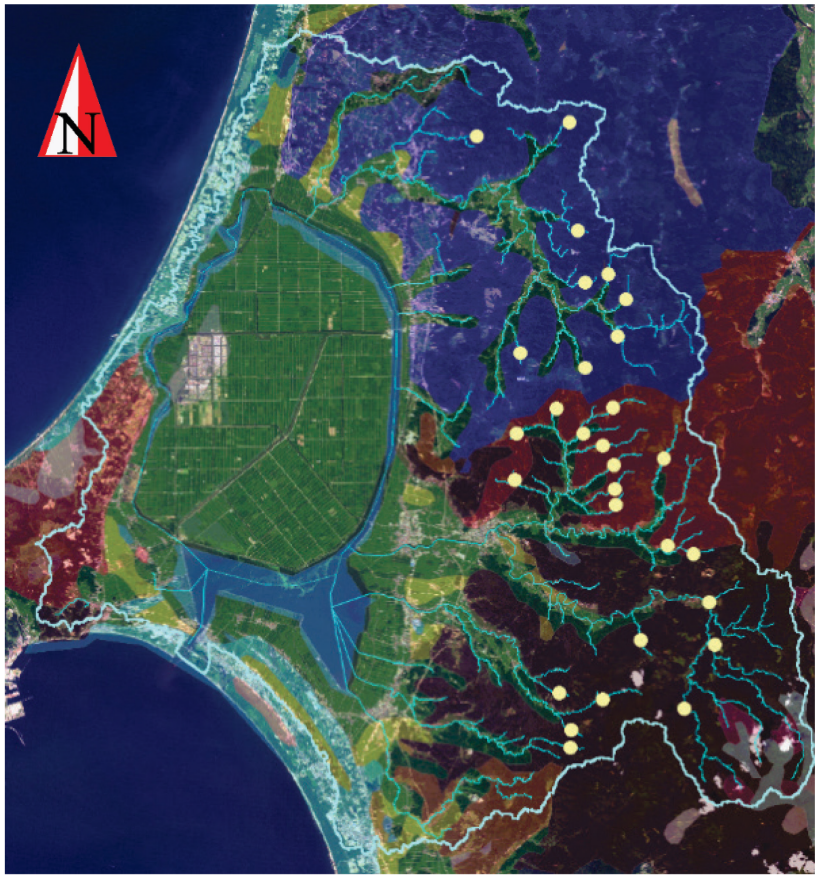

Fig. 2

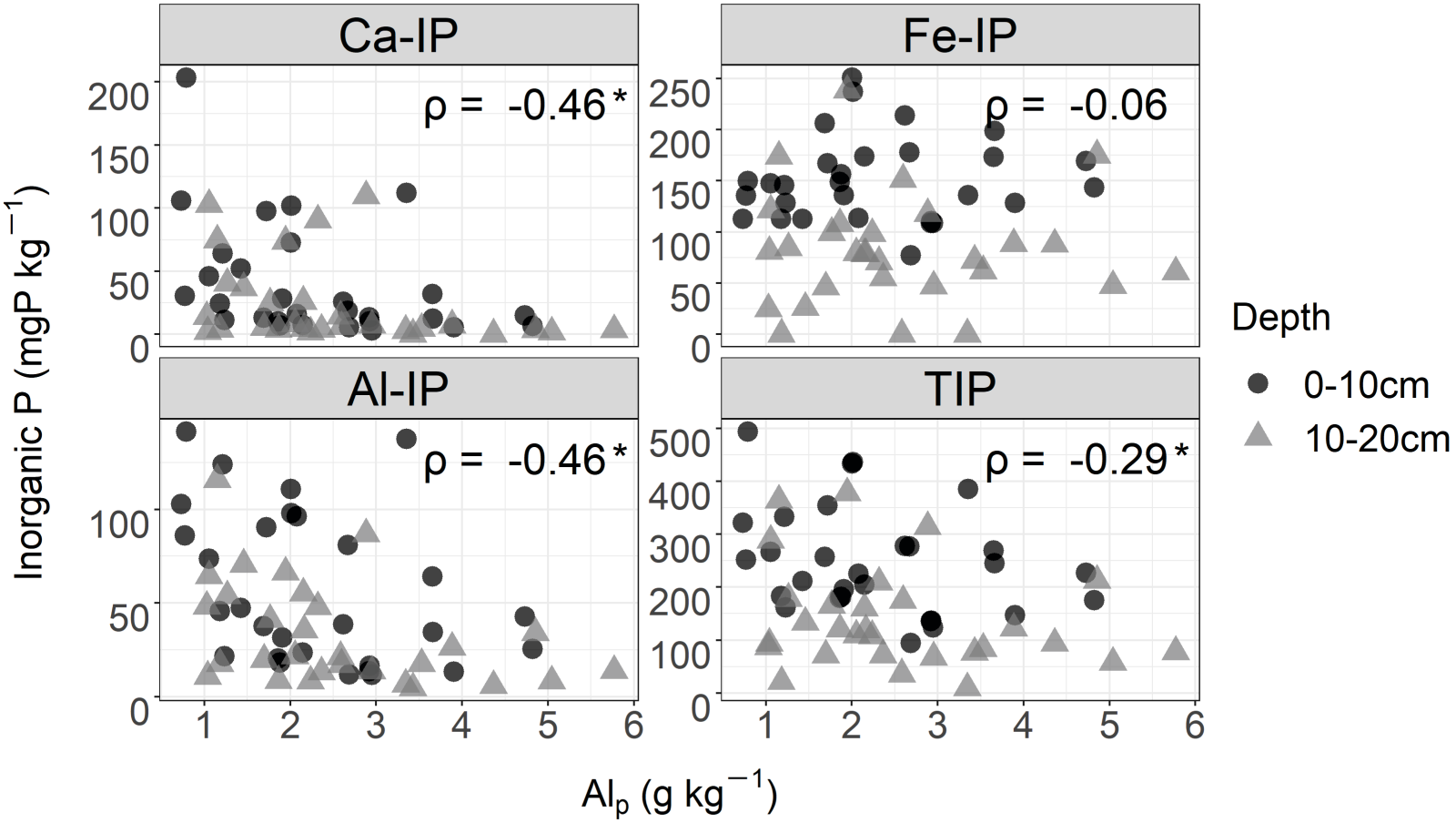
Ca-IP
ρ = -0.46*
Fe-IP
ρ = -0.06
Al-IP
ρ = -0.46*
TIP
ρ = -0.29*
Inorganic P (mgP kg^{-1})
Al$_p$ (g kg^{-1})
Depth
0-10cm
10-20cm

Fig. 3

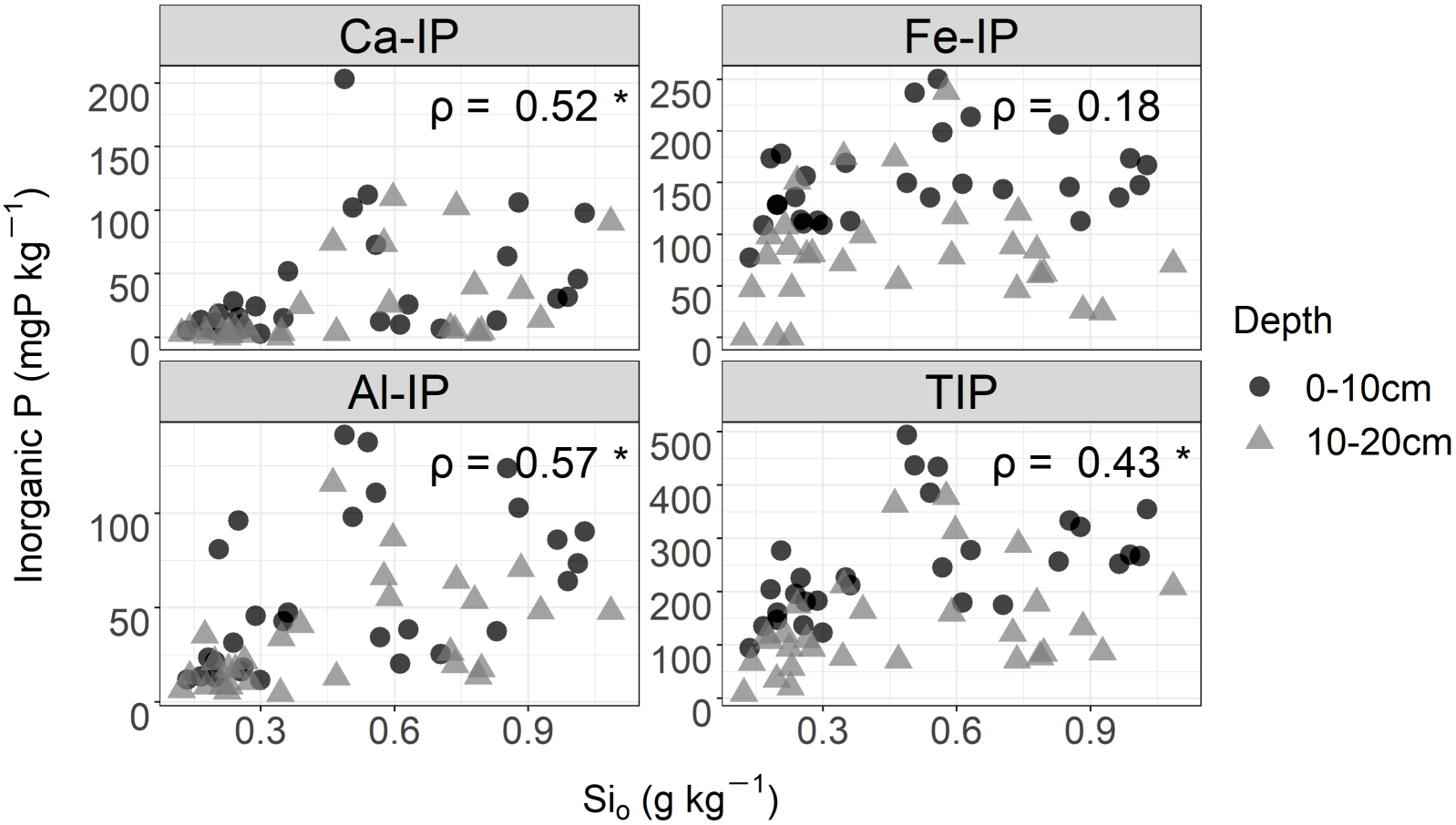
Ca-IP
ρ = 0.52 *
Fe-IP
ρ = 0.18
Al-IP
ρ = 0.57 *
TIP
ρ = 0.43 *
Inorganic P (mgP kg^{-1})
Si$_o$ (g kg^{-1})
Depth
0-10cm
10-20cm

Fig. 4

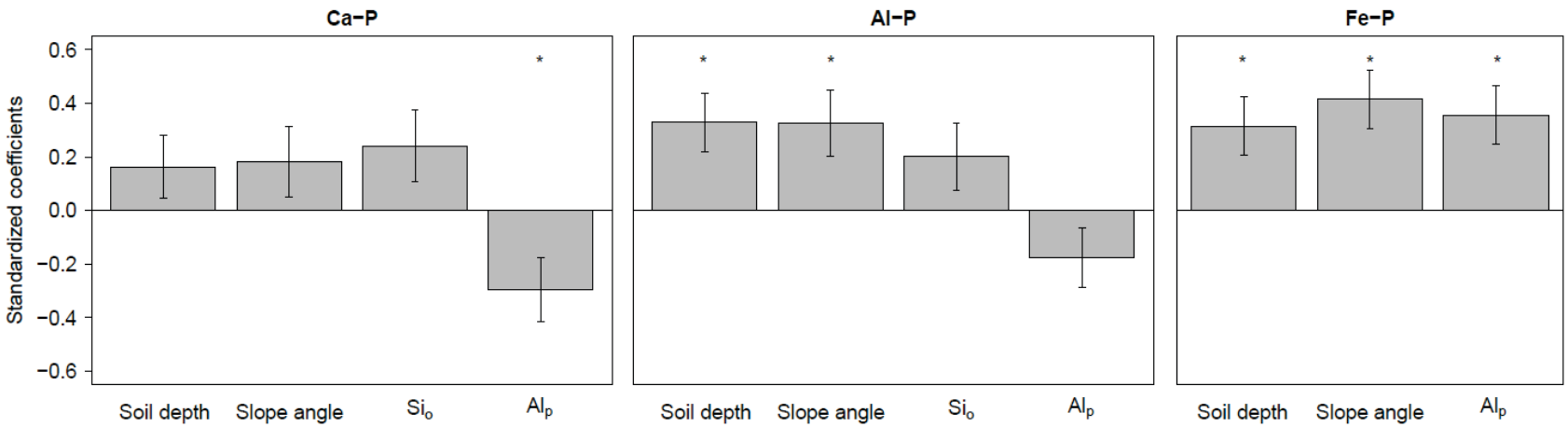
Ca−P
Al−P
Fe−P
Standardized coefficients
0.6
0.4
0.2
0.0
−0.2
−0.4
−0.6
*
Soil depth
Slope angle
Si$_o$
Al$_p$

Supplementary materials

Effect of active aluminum on soil phosphorus forms in a forested watershed in Akita, Japan

Nanae Hosokawa, Yuka Ozawa, Atsushi Hayakawa, Yuichi Ishikawa, Tadashi Takahashi

Table S1 Selective extracted Al, Fe and Si at 0–10 and 10–20 cm soil depths

	($g\ kg^{-1}$)		($g\ kg^{-1}$)		($g\ kg^{-1}$)		($g\ kg^{-1}$)		($g\ kg^{-1}$)		%		($g\ kg^{-1}$)				mol ratio	
	Al_o		Fe_o		Si_o		Al_p		Fe_p		$Al_o+1/2Fe_o$		Al_o-Al_p		Al_p/Al_o		$(Al_o-Al_p)/Si_o$	
	Depth (cm)		Depth (cm)		Depth (cm)		Depth (cm)		Depth (cm)		Depth (cm)		Depth (cm)		Depth (cm)		Depth (cm)	
ID	0-10	10-20	0-10	10-20	0-10	10-20	0-10	10-20	0-10	10-20	0-10	10-20	0-10	10-20	0-10	10-20	0-10	10-20
1	3.4	4.5	7.9	8.7	0.17	0.22	2.9	4.4	5.9	6.9	0.73	0.89	0.43	0.16	0.87	0.96	2.72	0.75
3	3.2	3.3	5.0	3.7	0.25	0.21	2.1	1.9	2.6	1.9	0.57	0.51	1.16	1.40	0.64	0.57	4.83	6.82
4	3.9	3.5	6.7	5.2	0.26	0.24	2.9	2.6	3.9	2.9	0.72	0.61	0.96	0.90	0.75	0.74	3.91	3.87
5	2.5	2.6	6.6	5.7	0.26	0.18	1.9	2.2	3.8	4.1	0.59	0.54	0.66	0.36	0.74	0.86	2.65	2.06
6	1.9	2.0	4.9	5.2	0.20	0.28	1.2	1.0	1.9	1.8	0.44	0.46	0.69	0.93	0.64	0.53	3.63	3.52
8	2.2	2.5	6.6	7.1	0.36	0.26	1.4	2.1	2.6	2.6	0.55	0.61	0.79	0.47	0.64	0.82	2.28	1.84
9	3.1	3.3	3.6	3.2	0.14	0.12	2.7	3.3	2.8	2.9	0.49	0.49	0.40	0.00	0.87	1.00	3.10	0.00
10	4.5	5.1	8.3	8.5	0.20	0.23	3.9	5.0	5.5	6.5	0.87	0.93	0.64	0.06	0.86	0.99	3.38	0.26
11	3.2	2.7	4.0	4.3	0.21	0.14	2.7	3.0	1.7	2.0	0.52	0.49	0.49	-0.20	0.84	1.07	2.49	-*
12	2.9	3.5	4.2	5.3	0.24	0.20	1.9	2.6	1.8	2.7	0.50	0.62	1.02	0.94	0.65	0.73	4.45	5.01
13	2.2	1.8	9.0	8.6	0.29	0.23	1.2	1.2	3.7	3.2	0.67	0.61	1.04	0.60	0.53	0.66	3.77	2.77
14	5.2	4.6	10.7	10.3	0.83	0.74	1.7	1.7	2.5	2.4	1.05	0.98	3.47	2.92	0.33	0.37	4.36	4.14
15	3.2	2.6	11.8	10.2	0.97	0.93	0.8	1.0	2.3	1.9	0.91	0.78	2.45	1.61	0.24	0.39	2.64	1.80
16	5.2	5.4	8.8	7.8	0.85	0.78	1.2	1.3	1.9	1.4	0.96	0.93	3.95	4.11	0.24	0.24	4.83	5.49
17	4.1	4.6	7.0	7.2	0.61	0.47	1.9	2.4	2.4	2.3	0.76	0.82	2.29	2.19	0.45	0.52	3.89	4.86
18	5.1	5.5	6.8	7.9	0.63	0.59	2.6	2.1	2.2	2.0	0.85	0.94	2.48	3.34	0.51	0.39	4.09	5.92
19	5.2	4.9	11.1	10.4	1.01	0.88	1.1	1.5	1.4	2.1	1.07	1.01	4.14	3.46	0.20	0.30	4.26	4.08
20	3.1	2.6	6.9	7.1	0.18	0.17	2.1	2.2	2.5	3.1	0.66	0.61	0.94	0.41	0.70	0.84	5.35	2.44
21	2.2	2.6	9.9	11.2	0.49	0.46	0.8	1.2	2.1	2.3	0.71	0.82	1.40	1.49	0.36	0.44	2.98	3.36
22	4.2	4.4	5.8	7.3	0.30	0.34	2.9	3.4	1.8	2.4	0.71	0.80	1.27	0.94	0.70	0.79	4.43	2.84
23	4.0	4.6	8.2	8.1	0.88	0.74	0.7	1.1	1.0	1.4	0.81	0.87	3.32	3.57	0.18	0.23	3.93	5.03
25	6.2	7.2	7.1	8.0	0.57	0.73	3.7	3.9	4.4	4.2	0.97	1.12	2.53	3.31	0.59	0.54	4.63	4.75
26	10.9	9.5	9.1	7.5	0.99	0.80	3.7	3.5	3.0	3.4	1.55	1.32	7.26	5.95	0.34	0.37	7.64	7.79
28	5.7	5.3	6.9	6.6	1.03	1.09	1.7	2.3	2.1	2.5	0.91	0.86	3.96	3.02	0.30	0.43	4.01	2.90
29	4.5	3.7	12.1	10.2	0.56	0.58	2.0	1.9	3.1	2.8	1.05	0.88	2.48	1.75	0.45	0.53	4.63	3.16
30	7.7	7.3	8.9	8.8	0.70	0.79	4.8	5.8	4.4	4.9	1.21	1.17	2.83	1.55	0.63	0.79	4.19	2.05
31	5.5	5.2	5.5	4.9	0.54	0.60	3.4	2.9	2.8	2.5	0.83	0.76	2.19	2.33	0.61	0.55	4.22	4.06
32	3.5	2.7	5.8	5.8	0.51	0.39	2.0	1.8	2.5	2.3	0.64	0.57	1.46	0.98	0.58	0.64	2.99	2.63
33	6.6	6.3	5.1	4.7	0.35	0.35	4.7	4.9	3.6	3.7	0.92	0.86	1.91	1.41	0.71	0.78	5.66	4.24

Al_o: oxalate extracted aluminum, Fe_o: oxalate extracted iron, Al_p: pyrophosphate extracted aluminum, Fe_p: pyrophosphate extracted iron, Si_o: oxalate extracted silicon, *: Negative value.

Table S2 Soil properties and soil P determined by Sekiya method at 0–10 and 10–20 cm soil depths

	(%) TC		(%) TN		pH (H_2O)		(mg kg^{-1}) Ca-IP		(mg kg^{-1}) Ca-OP		(mg kg^{-1}) Al-IP		(mg kg^{-1}) Al-OP		(mg kg^{-1}) Fe-IP		(mg kg^{-1}) Fe-OP	
	Depth (cm)		Depth (cm)		Depth (cm)		Depth (cm)		Depth (cm)		Depth (cm)		Depth (cm)		Depth (cm)		Depth (cm)	
ID	0-10	10-20	0-10	10-20	0-10	10-20	0-10	0-10	10-20	0-10	10-20	10-20	0-10	10-20	0-10	10-20	0-10	10-20
1	7.0	3.2	0.51	0.29	4.5	4.6	13	0	0	0	13	6	0	0	109	88	101	0
3	5.5	2.9	0.40	0.25	4.6	4.5	16	4	5	3	96	8	0	0	114	108	87	72
4	4.4	2.6	0.30	0.20	4.8	4.9	10	6	0	1	16	17	0	0	111	151	109	11
5	4.6	3.3	0.31	0.28	5.4	4.5	7	2	0	1	18	8	3	0	156	98	159	261
6	4.0	1.3	0.28	0.14	4.7	5.4	11	2	1	1	22	11	19	0	128	81	43	45
8	3.4	1.4	0.21	0.13	4.9	5.0	52	8	0	0	47	22	0	0	113	80	86	81
9	4.4	3.4	0.31	0.25	4.8	5.0	5	3	0	0	12	7	27	0	77	0	95	177
10	5.8	4.3	0.37	0.30	4.5	4.6	6	2	0	1	13	8	7	0	129	48	109	206
11	2.7	1.3	0.17	0.13	5.3	5.1	19	7	0	1	81	14	0	0	178	47	103	103
12	4.1	2.5	0.28	0.19	5.3	5.0	28	14	0	2	32	21	0	0	136	0	58	139
13	4.2	2.1	0.31	0.19	5.5	5.1	24	4	0	2	46	18	0	0	113	0	187	208
14	4.3	1.7	0.28	0.15	5.9	5.9	13	5	0	0	38	20	2	0	206	46	36	155
15	4.1	1.0	0.24	0.09	5.8	5.9	31	14	0	1	86	48	0	0	136	25	134	85
16	3.8	2.2	0.23	0.16	6.0	6.1	64	40	0	1	124	54	0	0	146	85	206	119
17	4.7	1.8	0.32	0.16	5.6	5.5	10	4	0	2	20	13	4	0	149	55	141	109
18	3.0	1.6	0.25	0.13	5.3	5.4	26	26	0	0	39	55	0	0	214	79	49	135
19	2.2	2.8	0.14	0.18	6.0	6.0	46	37	0	2	74	71	0	0	148	26	57	164
20	2.4	3.0	0.18	0.24	5.0	4.9	7	5	2	4	23	35	0	0	174	79	29	121
21	4.0	1.6	0.24	0.14	5.7	5.6	203	75	14	0	142	116	0	0	150	174	104	76
22	1.4	1.3	0.12	0.12	5.1	5.3	3	0	2	0	12	5	0	0	109	72	0	2
23	1.2	1.3	0.08	0.10	6.1	6.0	106	103	0	5	103	64	0	0	113	121	0	37
25	5.4	1.5	0.35	0.13	5.1	5.5	12	7	5	1	34	26	0	0	199	89	115	140
26	5.0	2.1	0.29	0.15	5.3	5.5	32	5	5	0	64	18	0	4	174	62	152	102
28	3.0	2.2	0.19	0.18	5.8	5.6	98	91	1	3	90	48	0	2	167	71	93	111
29	3.5	3.0	0.21	0.19	5.1	5.4	73	74	5	0	111	66	0	0	251	238	163	119
30	6.6	5.5	0.47	0.42	5.2	5.1	7	3	4	0	25	14	12	13	144	61	138	259
31	4.7	1.9	0.33	0.17	5.3	4.7	112	110	11	6	138	87	0	4	136	118	274	219
32	3.6	1.1	0.23	0.10	5.1	5.4	102	25	8	2	98	41	0	0	237	99	12	123
33	6.9	4.2	0.44	0.31	5.5	5.2	15	4	7	0	43	34	66	53	169	175	423	335

TC: total carbon, TN: total nitrogen, IP: inorganic phosphorus, OP: organic phosphorus.

Table S3 Soil P determined by Sekiya method at the 0–10 cm and 10–20 cm soil depths in the different soil areas

	(cm)	(mg kg^{-1})	(mg kg^{-1})	(mg kg^{-1})	(mg kg^{-1})	(mg kg^{-1})	(mg kg^{-1})
Soil area	depth	Ca-IP	Ca-OP	Al-IP	Al-OP	Fe-IP	Fe-OP
NAA	0-10	15 ± 14	0.8 ± 1.8a	35 ± 32	6.2 ± 10	124 ± 29a	99 ± 30
	10-20	4 ± 3	0.9 ± 0.8	11 ± 5a	0.1 ± 0.1	78 ± 43	106 ± 90
AA	0-10	47 ± 57	1.4 ± 3.9a	61 ± 43	0.5 ± 1.3	149 ± 34ab	83 ± 70
	10-20	27 ± 32	1.6 ± 1.7	43 ± 31b	0.0 ± 0.0	63 ± 50	112 ± 56
BFS	0-10	56 ± 45	5.7 ± 3.1b	75 ± 40	9.7 ± 23	184 ± 41b	171 ± 125
	10-20	40 ± 44	1.5 ± 2.0	42 ± 25b	9.5 ± 18	114 ± 63	176 ± 86

NAA: non-allophanic Andosols, AA: allophanic Andosols, BFS: Brown forest soils, IP: inorganic phosphate, OP: organic phosphate. Different cases indicate significant differences among the soil areas at each soil depth by multiple comparisons (Games-Howell test).

Table S4 Soil TP at 0–20 cm soil depth in the two lithological areas.

	Igneous rock	Sedimentary rock
Soil TP (mg kg^{-1}) *	1797 ± 624	1225 ± 401

Asterisk indicates the significant difference between the lithologies (Wilcoxon rank sum test, $p < 0.05$).

Table S5 Spearman's correlation (ρ) of soil TP at 0-20cm soil depth with topography and Sekiya TP at 0-20cm soil depth

Item	Elevation	Slope angle	Sekiya TP
Soil TP	0.51*	0.61*	0.83*

Asterisks indicate significant correlation ($p < 0.05$).

Table S6 Spearman's correlation (ρ) of selective extracted Al, Si and Fe or soil properties with topography.

Item	Elevation	Slope angle
Al_o	0.46*	0.47*
Si_o	0.49*	0.52*
Fe_o	0.06	0.05
Al_p	0.10	0.02
Fe_p	−0.05	−0.18
Al_o−Al_p	0.51*	0.58*
Al_p/Al_o	−0.36*	−0.44*
pH	0.37*	0.51*
TC	−0.10	−0.25
TN	−0.19	−0.17

Asterisks indicate significant correlation ($p < 0.05$).

Table S7 Spearman's correlations (ρ) among selective extracted Al, Si and Fe, and pH.

	Si_o	Al_p	Al_o-Al_p	Al_p/Al_o	Fe_o	Fe_p	pH
Al_o	0.58*	0.51*	0.68*	−0.29*	0.20	0.19	0.26*
Si_o	---	−0.28*	0.91*	−0.85*	0.56*	−0.29*	0.77*
Al_p	---	---	−0.22	0.62*	−0.29*	0.65*	−0.52*
Al_o-Al_p	---	---	---	−0.88*	0.46*	−0.32*	0.72*
Al_p/Al_o	---	---	---	---	−0.52*	0.54*	−0.80*
Fe_o	---	---	---	---	---	0.08	0.47*
Fe_p	---	---	---	---	---	---	−0.51*

Al_o: oxalate extracted aluminum, Si_o: oxalate extracted silicon, Al_p: pyrophosphate extracted aluminum, Fe_o: oxalate extracted iron, Fe_p: pyrophosphate extracted iron. Asterisks indicate significant correlation ($p < 0.05$).

Table S8 Spearman's correlation of selective extracted Al, Si and Fe or total soil P determined by Sekiya method with TC and TN.

Item	TC	TN
Al_o	0.19	0.12
Si_o	−0.14	−0.26*
Fe_o	−0.02	−0.11
Al_p	0.35*	0.41*
Fe_p	0.56*	0.63*
Al_o-Al_p	−0.09	−0.21
Al_p/Al_o	0.25	0.36*
Ca-P	0.00	−0.14
Al-P	0.12	−0.02
Fe-P	0.59*	0.53*

Asterisks indicate significant correlation ($p < 0.05$).

Table S9 Spearman's correlation (ρ) of inorganic and organic P determined by Sekiya method with topography or andic indicators.

Item	Slope angle	Al_o	Fe_o	Fe_p	Al_o-Al_p
Ca-IP	0.41*	0.10	0.21	−0.41*	0.53*
Al-IP	0.48*	0.13	0.30*	−0.38*	0.57*
Fe-IP	0.26*	0.13	0.06	−0.03	0.26*
Ca-OP	0.27*	0.10	−0.16	0.01	0.12
Al-OP	−0.07	0.21	−0.23	0.34*	−0.03
Fe-OP	0.22	0.26*	0.07	0.44*	0.07

IP: inorganic P, OP: organic P, TIP: total inorganic P, TOP: total organic P.
Asterisks indicate significant correlations ($p < 0.05$).

Table S10 Spearman's correlation (ρ) of sum of Ca, Mg, K and Na contents with Elevation

Element	Depth	Elevation
Ca	0-10cm	0.50*
	10-20cm	0.49*
Mg	0-10cm	0.47*
	10-20cm	0.45*
K	0-10cm	−0.34
	10-20cm	−0.54*
Na	0-10cm	0.54*
	10-20cm	0.38*

Asterisks indicate significant correlation ($p < 0.05$).

Caption of Supplementary figures

Fig. S1 Relationship between Ca-P, Al-P, Fe-P, TIP, and Al_p/Al_o at soil depths of 0–10 cm and 10–20 cm. Asterisks indicate significant correlations ($p < 0.05$).

Fig. S2 Relationship between sum of Ca + Mg + K + Na at 0–20cm soil depth and elevation. Asterisk indicates a significant correlation ($p < 0.05$).

Fig. S3 Relationship between soil TP and sum of Ca + Mg + K + Na at 0–20cm soil depth. Asterisk indicates a significant correlation ($p < 0.05$). The difference of alkaline minerals between lithological areas was insignificant (Wilcoxon rank sum test, $p = 0.15$).

Fig. S1

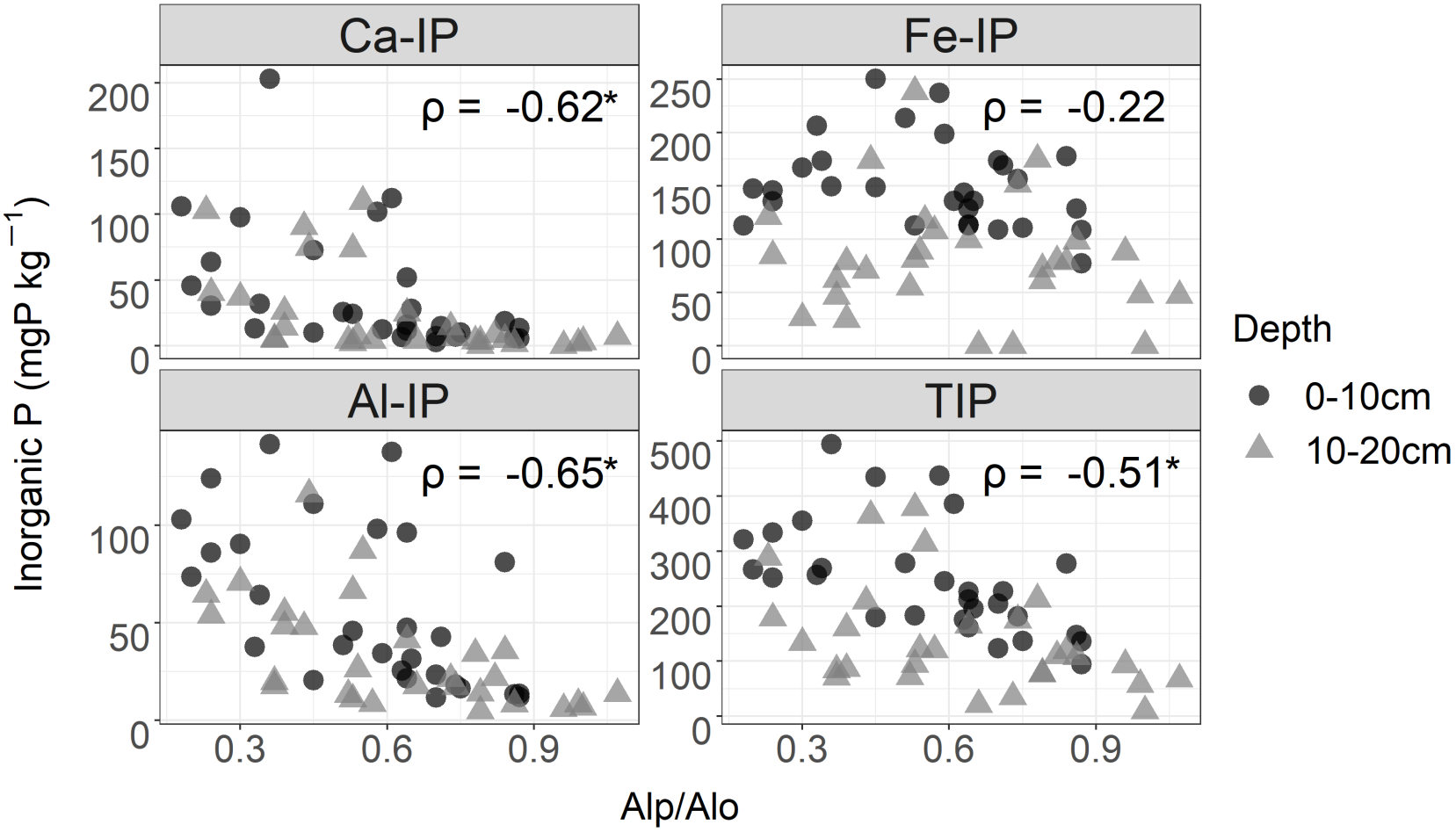
Ca-IP
ρ = -0.62*
Fe-IP
ρ = -0.22
Al-IP
ρ = -0.65*
TIP
ρ = -0.51*
Inorganic P (mgP kg^{-1})
Alp/Alo
Depth
0-10cm
10-20cm

Fig. S2

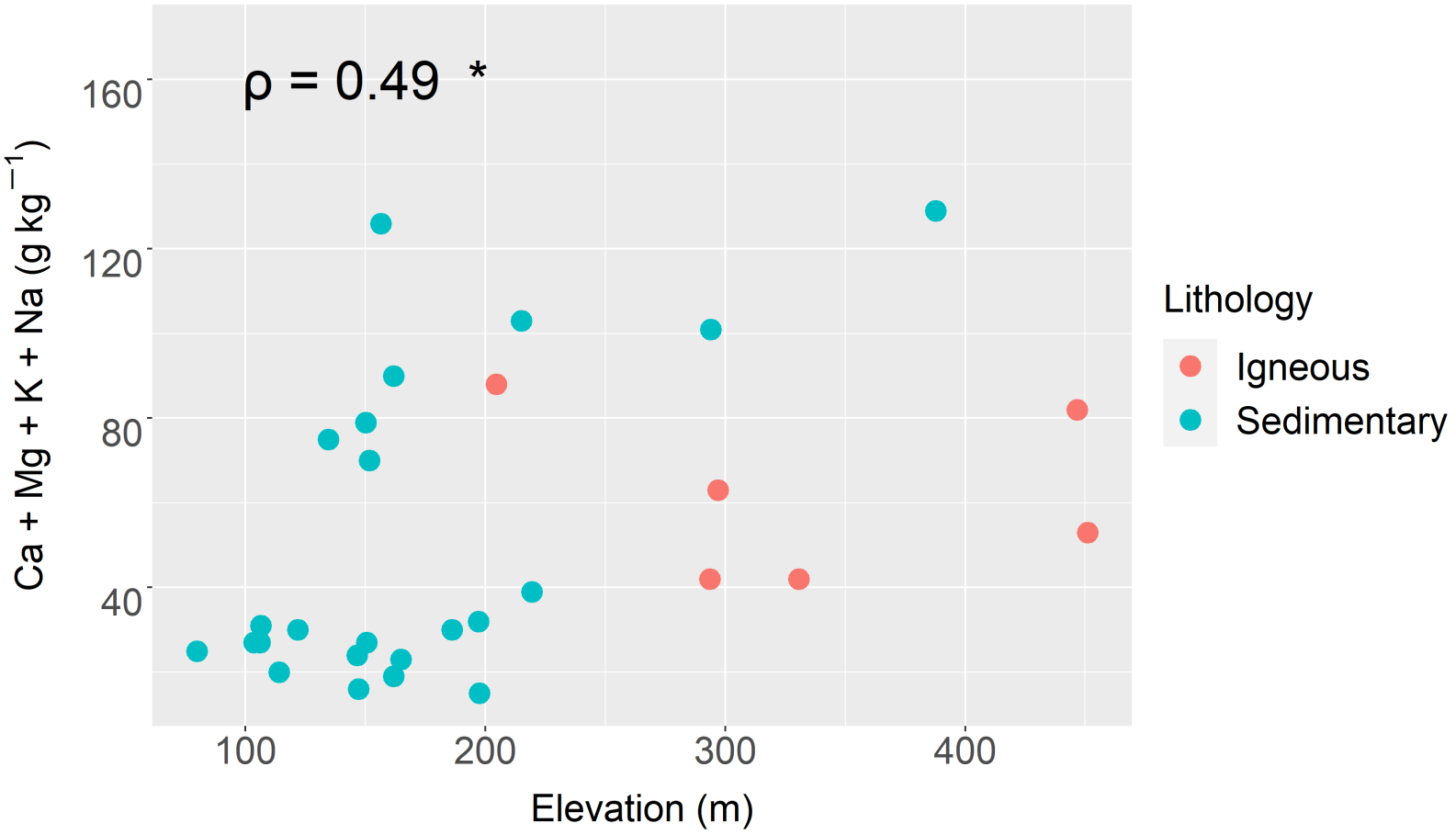
ρ = 0.49 *
160
120
80
40
Ca + Mg + K + Na (g kg^{-1})
100
200
300
400
Elevation (m)
Lithology
Igneous
Sedimentary

Fig. S3

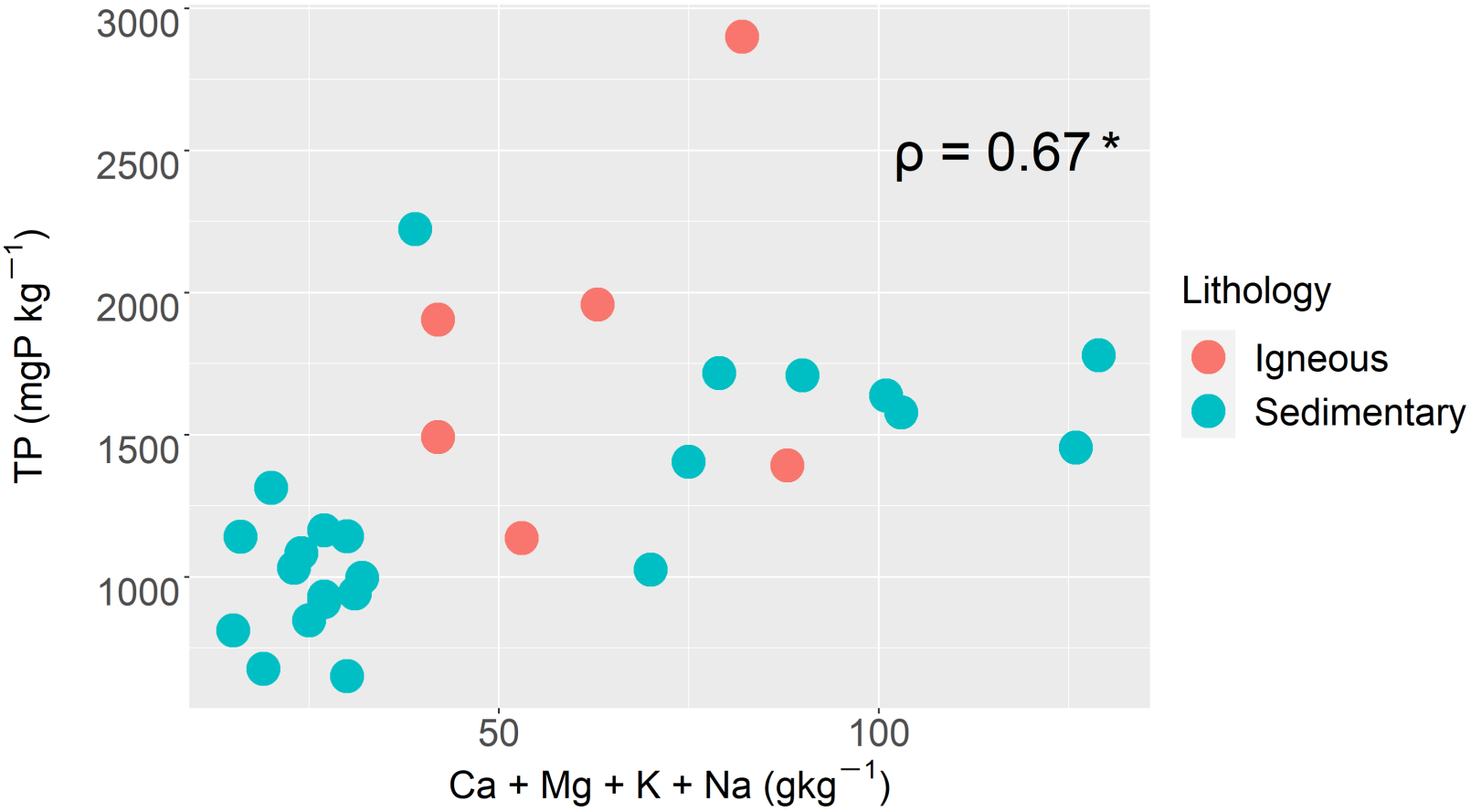
3000
2500
2000
1500
1000
TP (mgP kg^{-1})
ρ = 0.67 *
50
100
Ca + Mg + K + Na (gkg^{-1})
Lithology
Igneous
Sedimentary